buildings

MDPI

Article

Analysis of Energy-Saving Transport Conditions of Light-Particle Slurry

Xiaochun Wang [1], Fan Wang [1], Jun Li [1], Ye Zhang [1] and Lianjin Zhao [2,*]

[1] School of Environmental Science and Engineering, Suzhou University of Science and Technology, Suzhou 215009, China; sprdawn@usts.edu.cn (X.W.); 2013022048@post.usts.edu.cn (F.W.); lijun830@usts.edu.cn (J.L.); 1913022027@post.usts.edu.cn (Y.Z.)
[2] College of Civil Engineering and Architecture, Jiaxing University, Jiaxing 314001, China
* Correspondence: zlj@zjxu.edu.cn

Abstract: Ice slurry, as a new environmentally friendly cold storage medium, is widely used in the field of cold storage and air conditioning because of its excellent flow and heat transfer characteristics. Based on experimental data of slurry flow, the rheological properties of light-particle slurries composed of polyethylene particles and water were analyzed using the response surface method. Using the yield stress and viscosity as the responses and considering three key influencing factors (solid-phase content, particle size, and pipe diameter) simultaneously, the order and law influencing the rheological factors were found. This was a new attempt to find energy-saving conditions for light slurry particle transport using the response surface method. The results showed that the response surface method can select the minimum working condition of mixed slurry viscosity and yield stress to ensure the safe and energy-saving transport of slurry. Moreover, it was also found that the main factor influencing slurry yield stress is the pipe diameter, and the yield stress increases with increasing pipe diameter. The main factor influencing slurry viscosity is particle size, and the viscosity increases with increasing particle size.

Keywords: ice slurry; response surface method; rheological properties; transport conditions; energy-saving

Citation: Wang, X.; Wang, F.; Li, J.; Zhang, Y.; Zhao, L. Analysis of Energy-Saving Transport Conditions of Light-Particle Slurry. *Buildings* **2023**, *13*, 894. https://doi.org/10.3390/buildings13040894

Academic Editors: Christopher Yu-Hang Chao and Chi-Ming Lai

Received: 3 March 2023
Revised: 19 March 2023
Accepted: 23 March 2023
Published: 28 March 2023

1. Introduction

Ice slurry, also known as "binary ice", is a solid–liquid two-phase fluid consisting of water, ice particles, and a freezing point regulator, with an average diameter of ice crystal particles not exceeding 1 mm [1,2]. Compared to conventional chilled water, ice slurry has a larger cooling capacity per unit volume, and its cooling capacity is 5–6 times higher [3], allowing it to respond to changes in a cold load more quickly [4]. At the same time, ice slurry as a storage medium is one of the effective means to achieve "peak-shifting and valley-filling" of the power grid [5]. With the increasing global warming phenomenon, Dodoo's [6] analysis shows that the demand for cooling energy in buildings will increase significantly. The application of phase change energy storage materials such as ice slurry is considered an effective way to improve energy management and energy efficiency in buildings [7]. The CAPCOM building in Osaka, Japan, as a representative building that currently uses an ice slurry storage air conditioning system [8], uses ice slurry as the storage medium, which results in a significant improvement in cooling efficiency, reduction in equipment size and power consumption, and savings in initial investment and operating costs.

As a solid–liquid two-phase flow fluid, ice slurry will exhibit the characteristics of a non-Newtonian fluid when the ice content rate reaches a certain value due to the presence of solid-phase particles [9–11]. For non-Newtonian fluids, Monteiro et al. [12] summarized four non-Newtonian rheological models commonly used for solid–liquid two-phase flows in pipes: the Bingham model, the power-law model, the Herschel–Bulkley model (H–B model), and the Casson model. Onokoko et al. [13] found that the flow of

propylene glycol ice slurry in the laminar flow region meets the characteristics of the Bingham model. Mika et al. [14] analyzed the rheological properties of a 10.6% glycol ice-slurry solution and found that the rheological properties of ice slurry depend on the shear rate: when the shear rate is low, the ice slurry behaves as Bingham fluid; when the shear rate is large, the power-law model is more consistent. Illán [15] et al. analyzed the rheological properties of a 9% NaCl ice-slurry solution and found that the rheological law of the H–B model was satisfied at lower and higher shear rates, while the rheological law of the intermediate section deviated from the H–B model. At present, the research on the rheological properties of ice slurry is still immature. To better apply ice slurry for cold storage and to better use ice slurry in the flowing environment, the rheological properties of ice slurry still need to be researched further. However, during the storage and transport of ice slurry, there are a series of kinetic behaviors, such as agglomeration, Ostwald ripening, and fragmentation of ice crystals [16,17], and the size and distribution of ice crystal particles change with time, which in turn have an impact on the flow and heat transfer of ice slurry [18]. Therefore, in order to accurately study the effect of particle size on the rheological properties of light slurry particles, we chose a mixed slurry composed of polyethylene particles and water, instead of ice slurry, for flow experiments. In addition, yield stress and viscosity are important parameters in the rheological properties of the slurry, and their magnitude can affect the safety and economy of the slurry transport. So the yield stress and viscosity were used as the responses in the response surface method.

Chai et al. [19], based on the response surface method, optimized the distribution of air distribution of the fan, and the results showed that the uniformity of airflow at the outlet of the optimized fan was significantly improved; when the height from the central plate blade was 5%, the pressure drop of the impeller was reduced by 37.78%, and the delivery performance of the fan was improved. Zhu et al. [20] analyzed the factors affecting the yield stress and viscosity of coal gangue backfill using the response surface optimization design method and evaluated the interaction between the factors. Alkalbani et al. [21] used the response surface optimization design method to analyze the gel strength, yield stress, and viscosity of water-based mud, and found that zinc oxide nanoparticles can better maintain the rheological properties of the slurry, and optimized its optimal concentration. At present, the response surface method has been successfully used for the optimal design of various equipment performance parameters and the study of the rheological properties of mixture slurry and its ratio optimization; however, it has rarely been used for the study of the rheological properties of a solid–liquid two-phase flow of ice slurry with light particles (with a solid–liquid density ratio of less than 1).

Ice slurry is widely used in the fields of building cold storage, food processing, and medical protection [22], and the requirements for pipe diameter, particle size, and solid-phase content vary from field to field. Unreasonable operating conditions of the slurry will not only lead to pipe wear and clogging but also increase the conveying resistance and improve the energy consumption of the system. Therefore, in order to ensure more stable, efficient, and energy-saving transport of ice slurry, we need to consider the influence of pipe diameter, particle size, and solid-phase content on yield stress and viscosity, and establish a proper analysis method so that the best working conditions can be selected according to the engineering reality. Given this, a mixed slurry composed of polyethylene particles and water was selected for our experiment. The flow experiment was carried out in a horizontal circular tube to obtain the shear stress and shear rate of the light-particle mixed slurry and to determine the appropriate rheological equation. Based on the response surface method, the influence of pipe diameter, particle size, and solid content on the rheological parameters was analyzed. At the same time, the influence of the interaction of pipe diameter, particle size, and solid content on the rheological parameters was also analyzed. Finally, based on experimental measurement, the energy-saving condition of light-particle mixed slurry transportation was determined using the response surface method, with the minimum yield stress and viscosity as the objective.

2. Experimental Materials and Devices

2.1. Solid and Liquid Phase Working Medium

In order to study the effect of particle size of the solid phase on the flow characteristics of slurry, polyethylene particles (with a density of 922 kg/m^3) with a density similar to ice crystal particles (with a density of 920 kg/m^3) were used in the experiment. Three variations of polyethylene particles with an average particle size of 0.3 mm, 0.4 mm, and 0.5 mm were obtained by screening polyethylene through a screen mesh. Figure 1 shows a physical image of the polyethylene particles in three particle sizes under the microscope. The liquid-phase working medium was pure water, and the addition of a surfactant to the slurry made the polyethylene particles achieve a dispersion effect similar to the ice-slurry flow in the flow process. After many tests in the early stage, it was found that adding 0.025 vol% of sodium dodecyl sulfate (SDS) per 5 vol% solid content for the experiment had the best effect.

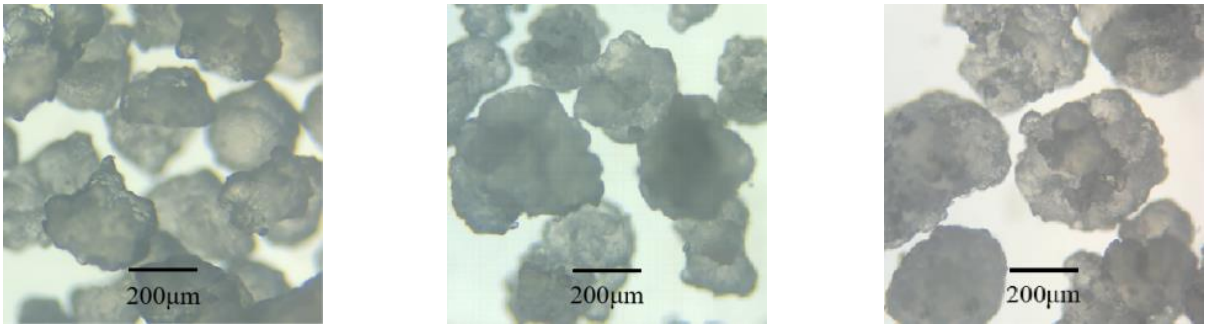

(**a**) (**b**) (**c**)

Figure 1. The physical picture of polyethylene particles: (**a**) particle size = 0.3 mm; (**b**) particle size = 0.4 mm; and (**c**) particle size = 0.5 mm.

2.2. Experimental Devices

The experimental device is shown in Figure 2. The experimental device was composed of three parts: the refrigerant circulation system, the pressure-drop test system, and the data acquisition system. Figure 3 shows an image of the experimental device. The constant-temperature circulating water tank provides a constant low-temperature environment for the ice-slurry flow during the experiment (model DL-3030, Shanghai Qixun Instrument company). The controllable temperature range was −30 to 50 °C, and the cooling capacity was 1000–3000 W. The pressure-drop test system is composed of a storage tank, mixing motor, circulating pump, electromagnetic flowmeter, test pipe section, thermocouple, differential pressure transmitter, and pressure sensor. The ice-slurry storage device is a stainless steel tank with an outer diameter of 80 cm, an inner diameter of 60 cm, and a height of 100 cm. The top is equipped with a feeding port to facilitate the addition of experimental materials. The specific parameters of other experimental equipment are shown in Table 1. The data acquisition system adopts the intelligent equipment monitoring module produced by Changsha Zhongdeng Company, which can display, record, and save all of the measured parameters in the experiment process in real time, and the recording time interval was 10 s. The test tube section is composed of a transparent plexiglass round tube and a round copper tube. The total length of the pressure-drop test section is 1 m and 0.9 m. Thermocouples are inserted at the front and rear ends to record the fluid temperature in real time. The test tubes are placed horizontally and are insulated with cotton, rubber, and plastic insulation.

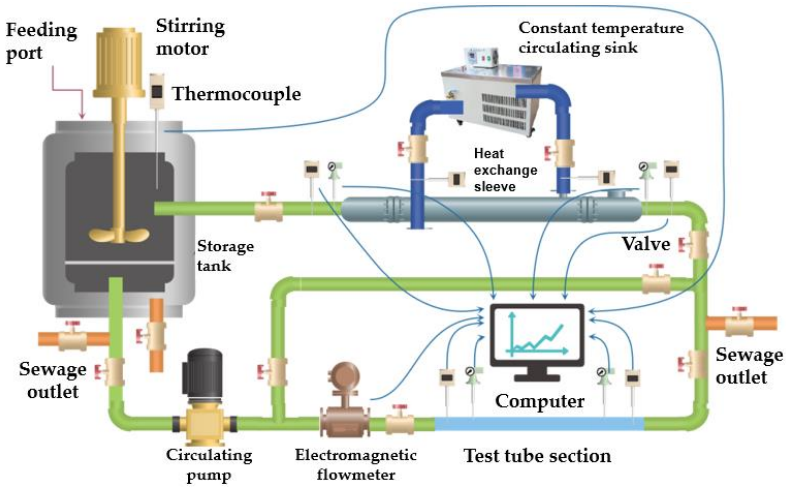

Figure 2. Schematic diagram of the experimental device.

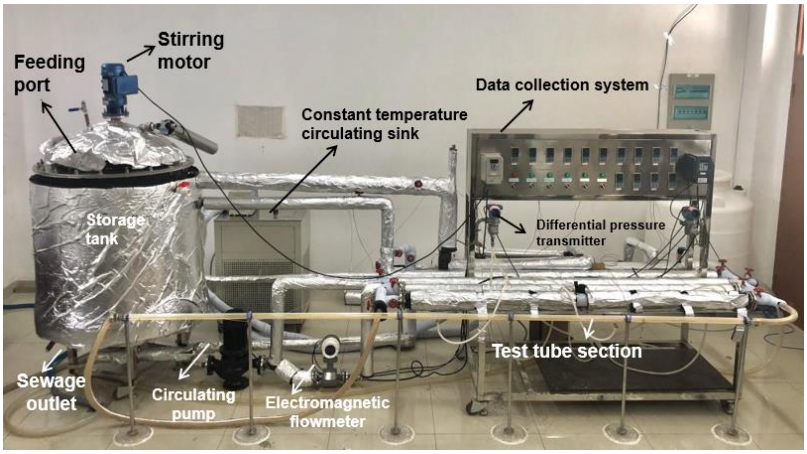

Figure 3. The physical layout of the experimental device.

Table 1. Specific parameters of the experimental equipment.

Equipment Name	Product Model	Specifications	Company
Stirring motor	BLD09-11-0.75	Speed: 150 r/min	Yixing Yuanjia Environmental Protection Equipment (Yixing, China)
Circulating pump	25GW8-22	Speed: 2900 r/min; Rate of flow: 8 m^3/h; Lift: 22 m	Kaiping Danai Pump Manufacturing Co., Ltd. (Kaiping, China)
Electromagnetic flowmeter	TBD-20Y-F4-1-A-1-16-A	Range: 0–6 m^3/h; Precision: ±0.5%	Dalian Measuring Machinery Co., Ltd. (Dalian, China)
Differential pressure transmitter	3051CD2A22B1AB415M5HR5	Range: 0–30 kPa; Precision: ±0.06%	Emerson Electric Company (St. Louis, MO, USA)
Thermocouple	K-type	Precision: ±0.1 °C	Shanghai No. 3 Electric Instrument Factory (Shanghai, China)
Pressure-drop sensor	PCM300	Range: 0–100 kPa; Precision: ±0.5%	Suzhou Xuansheng Instrument Technology Co., Ltd. (Suzhou, China)

2.3. Test Process and Working Conditions

First, the storage tank was filled with pure water until it was about 10 cm above the mixing blade, and then a high-precision electronic balance (product model: CP512C, accuracy: ±0.01 g) was used to weigh a certain amount of SDS, which was poured into the storage tank using the feeding port. Then, the mixing motor was turned on, the speed was adjusted to 150 r/min, and the SDS solution was mixed in the storage tank as the liquid-phase working medium for the experiment. The circulating pump and exhaust pipe of the differential pressure transmitter were adjusted until the differential pressure transmitter reading was stable. The thermostatic water tank flow was used to control the temperature of the experiment. To simulate the real ice-slurry flow and prevent the solution from freezing, the temperature was controlled to about 3 °C. Then, an electronic meter was used to weigh a certain amount of polyethylene particles, which were then added and stirred for 2–3 min to form an ice-slurry solution. Finally, the flow valve was adjusted to control the flow rate, and the pressure-drop changes at each flow rate were observed and recorded. The specific test conditions are shown in Table 2.

Table 2. Test conditions.

Name	Working Condition Parameters
Flow velocity: v/m·s^{-1}	0.1~1 (Conduct an experiment every 0.1 m/s)
Pipe diameter: D/mm	17, 24 and 28 mm
Solid particle size: d/mm	0.3, 0.4 and 0.5 mm
Solid content (IPF): C_v/vol%	5, 10, 15 and 20 vol%

2.4. Error Analysis

The directly measured values during the experiment were the mass of polyethylene particles m, the length of pipe section L, the inner diameter of pipe D, the temperature T, the volume flow V, and the flow pressure drop ΔP. The mass of polyethylene particles m was measured using an electronic scale with an absolute error of 0.001 g. The length L of the pipe section was measured with a ruler, and the absolute error was less than 0.1 mm. The inner diameter D of the pipe was measured with a vernier caliper, and the absolute error was less than 0.1 mm. Temperature T was measured using a thermocouple with an absolute error of 0.1 °C. The volume flow V was measured using an electromagnetic flowmeter with an absolute error of 0.5% m^3/s. The flow pressure drop ΔP was measured using a differential pressure transmitter, and the absolute error was 0.06% Pa.

Indirectly measured values included flow velocity v, resistance coefficient λ, shear stress τ, and shear rate γ. The error transfer formula is as follows:

$$\delta_N = \sqrt{\sum_{i=1}^{n} \left(\frac{\partial N}{\partial x_i}\delta x_i\right)^2} \quad (1)$$

where N represents the indirect measurement value, $x_1, x_2, x_3, \ldots, x_n$ represents mutually independent measured values, δ_N represents the absolute error of the indirect measurement value, and δ_x is the absolute error of the direct measurement value. The relative error of the indirect measurement value is δ_N/N. The relative errors of flow velocity v, resistance coefficient λ, shear stress τ, and shear rate γ were 0.51%, 0.51%, 0.06%, and 0.50%, respectively.

3. Theory of Rheological Model

Ice slurry is generally considered a non-Newtonian fluid due to the existence of solid and liquid working mediums. At present, the rheological models describing non-Newtonian fluids include the Bingham model, the power-law model, the Herschele–Bulley (H–B model), and the Casson model, and their rheological models and curves are shown in Figure 4.

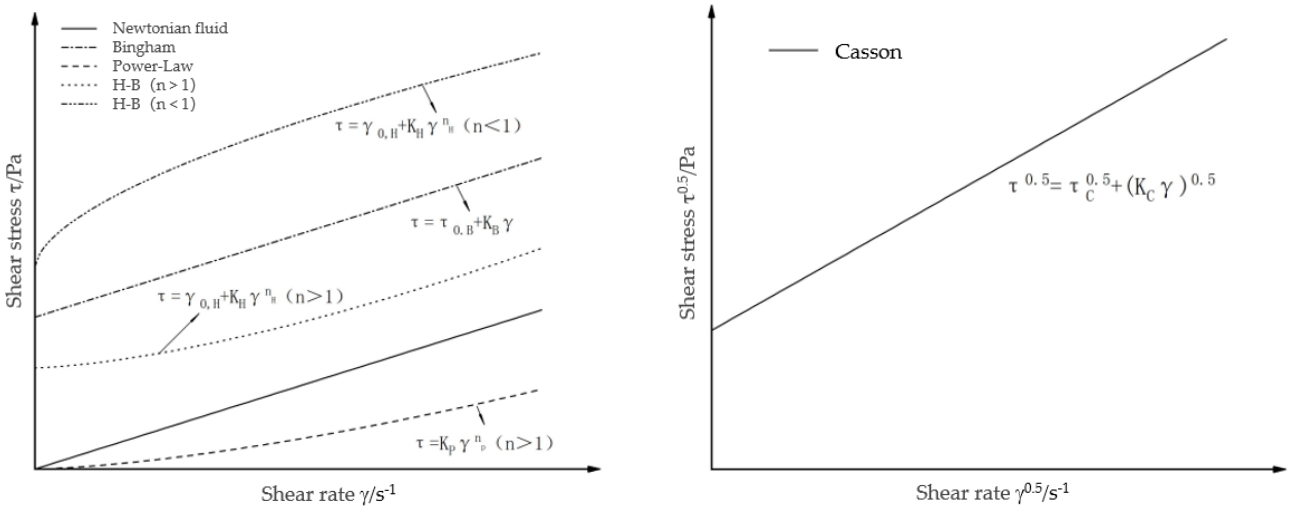

(**a**) (**b**)

Figure 4. Rheological curves of Newtonian fluid and four non-Newtonian fluid rheological models. (**a**) Newtonian fluid, the Bingham model, the power-law model, and the H–B model; and (**b**) the Casson model.

When ice slurry flows in the pipe, the shear stress τ and shear rate γ meet the following relationship:

$$\tau = \frac{D\Delta P}{4L} \tag{2}$$

$$\gamma = \frac{8v}{D} \tag{3}$$

In the above models, K is plastic viscosity, and its value reflects the viscosity of the ice slurry. n is the rheological index, and its value reflects the shear deformation behavior. When $n > 1$, the slurry shows shear thickening. When $n = 1$, the slurry acts as a Bingham fluid. When $n < 1$, the slurry shows shear thinning.

4. Analysis of Experimental Results and Response Surface Method

4.1. Rheological Model of Light-Particle Slurry

According to the experimental measurement results, when the inner diameter of the horizontal circular tube was 28 mm, the average solid particle sizes were 0.3 mm, 0.4 mm, and 0.5 mm, and the solid content was 5 vol%, 10 vol%, 15 vol% and 20 vol%, the relationship between shear stress and the shear rate is summarized in Figure 5. It can be seen from Figure 5 that the shear stress generally increases with increasing shear rate; the increased amplitude is also increasing, and the intercept of the left end on the Y-axis is not 0. This changing trend was consistent with the rheological characteristics of the H–B model. The use of the H–B model was proposed to fit the rheological curve of the mixed slurry. The obtained rheological equation is shown in Figure 5, and the fitting correlation was greater than 0.996. Therefore, for the light-particle solid–liquid two-phase flow with a solid–liquid density ratio of 0.922, the H–B model could reflect the rheological characteristics of the mixed slurry. In addition, the rheological index n was greater than 1, which indicated that the rheological relationship of the mixed slurry was an expansive plastic fluid with yield stress.

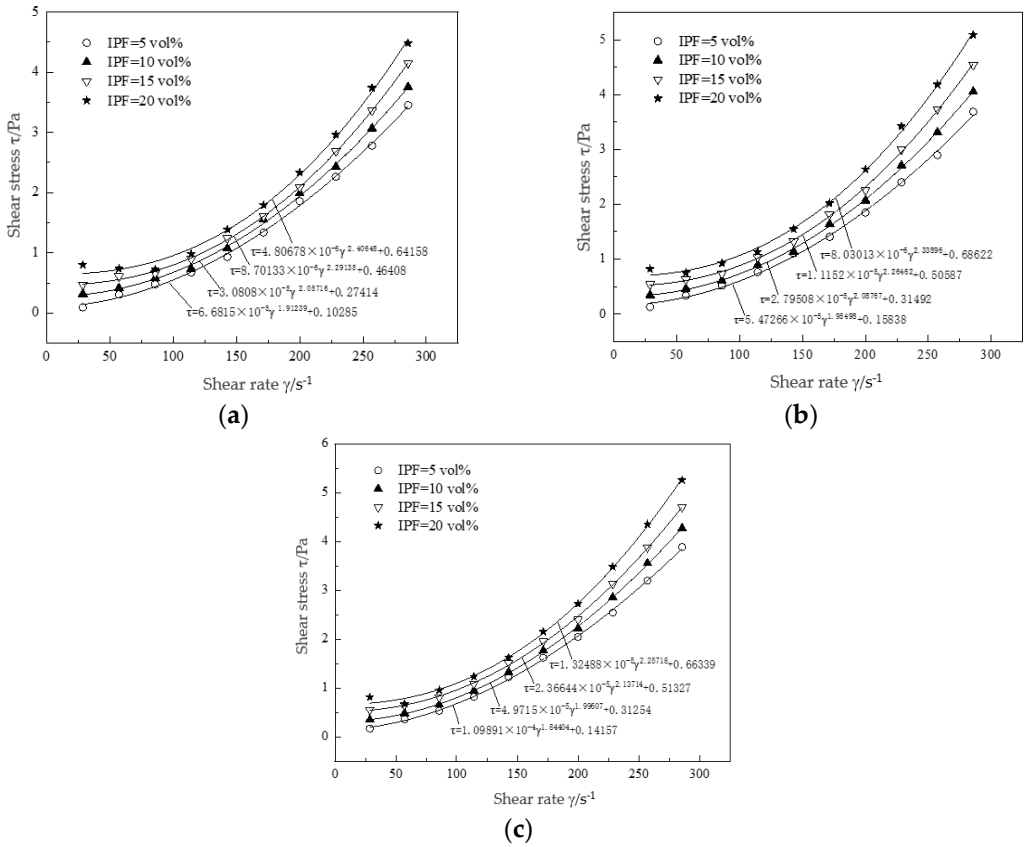

Figure 5. H–B model fitting curve under various working conditions when the pipe diameter was 28 mm: (**a**) particle size = 0.3 mm; (**b**) particle size = 0.4 mm; and (**c**) particle size = 0.5 mm.

4.2. Quadratic Regression Equation of Yield Stress and Viscosity

The response surface method (RSM), also known as regression design, is an experimental design that combines mathematical and statistical knowledge, uses multiple quadratic regression equations to fit the functional relationship between influencing factors and objectives, and analyzes the level and interaction of influencing factors by establishing a surface model of influencing factors. Our experiment was designed to analyze the independent or coupling influence of the influence factors (pipe diameter, particle size, solid content, and other variables) on the response targets (yield stress and viscosity).

In the H–B rheological equation, K is called plastic viscosity. The value of plastic viscosity will depend on the change in the rheological index n. Its value cannot directly reflect the magnitude of the viscosity of the paste, and even has an order of magnitude difference. Therefore, the discussion of viscosity cannot depend on the parameters obtained by fitting the H–B model. Based on this, the concept of differential viscosity is introduced, that is, the magnitude of tangent slope at a point on the rheological curve. Since the value of differential viscosity will change with the change in shear rate, the differential viscosity at the critical flow rate under each working condition is selected as the average viscosity of the ice slurry for discussion. In the following, differential viscosity is called viscosity for short.

In this paper, the pipe diameter D, particle size d, and solid content C_v were selected as the influencing factors, and the yield stress τ_0 and viscosity of the slurry μ_d were taken as the response values to carry out the three factors and three levels of the Box–Behnken Design (BBD) with three factors and three levels. The BBD method is a common analysis method of the response surface method. When the factors were the same, the number of BBD tests was less. The test consisted of 13 factorial tests and 4 repeated tests. A repeat test was used to determine test error and data repeatability. The test factors and levels are shown in Table 3. The three-level factors are the values of the three variables (i.e.,

the experimental condition variables) taken for each influencing factor. Design Expert 8.0 software was used to design the test scheme table, as shown in Table 4. The yield stress and viscosity values in Table 4 were obtained from the experimental measurement of pressure drop and the analysis of the slurry rheological model, and the variation in its values with different working conditions were analyzed.

Table 3. Table of test factors and coding level.

Factor	Coding	Level		
		−1	0	1
Pipe diameter/mm	D	17	24	28
Particle size/mm	d	0.3	0.4	0.5
Solid content/vol%	C_v	5	10	15

Table 4. Test design scheme.

Test Number	Pipe Diameter D/mm	Particle Size d/mm	Solid Content C_v /vol%	Yield Stress τ_0 /Pa	Viscosity μ_d /Pa·s
1	28	0.5	10	0.31254	0.01390
2	28	0.4	15	0.50587	0.01340
3	24	0.4	10	0.27542	0.01109
4	24	0.4	10	0.27542	0.01109
5	24	0.4	10	0.27542	0.01109
6	17	0.5	10	0.15963	0.00916
7	24	0.3	5	0.11088	0.00872
8	24	0.4	10	0.27542	0.01109
9	28	0.3	10	0.27414	0.00701
10	28	0.4	5	0.15838	0.00987
11	17	0.3	10	0.06039	0.00762
12	24	0.3	15	0.30113	0.01135
13	17	0.4	5	0.00058	0.00738
14	24	0.5	5	0.26417	0.01133
15	24	0.5	15	0.38912	0.01886
16	17	0.4	15	0.17272	0.01006
17	24	0.4	10	0.27542	0.01109

The response function relationships of the three independent variables in this test can be expressed by the following quadratic polynomial model:

$$y = \beta_0 + \sum_{i=3}^{n} \beta_i x_i + \sum_{i=3}^{n} \beta_{ij} x_i x_j + \sum_{i=3}^{n} \beta_{ii} x_i^2 + \xi \tag{4}$$

where y was the response value of yield stress and viscosity; β_0 represented a constant term, β_i was the coefficient of the x_i term; x_i and x_j represented three independent variables: pipe diameter, particle size, and solid content; β_{ij} was the coefficient of the interaction term.; β_{ii} was the coefficient of the quadratic term; and ξ indicated the error item.

According to the data in Table 4, multiple quadratic regression fitting was performed for Formula (4), and the response functions of yield stress and viscosity were shown in Formulas (5) and (6):

$$\begin{gathered}\tau_0 = 0.25 + 0.11D + 0.049\mathrm{d} + 0.1\mathrm{C_v} - 0.011\mathrm{Dd} + 0.036D\mathrm{C_v} \\ -0.016\mathrm{dC_v} - 0.039D^2 - 0.008404\mathrm{d}^2 - 0.0006914\mathrm{C_v}^2\end{gathered} \tag{5}$$

$$\begin{gathered}\mu_\mathrm{d} = 0.0075 + 0.00184D - 0.087\mathrm{d} - 0.0017\mathrm{C_v} + 0.0024D\mathrm{d} + \\ 0.000012D\mathrm{C_v} + 0.00245\mathrm{dC_v} - 0.00006D^2 + 0.036\mathrm{d}^2 - 0.0000446\mathrm{C_v}^2\end{gathered} \tag{6}$$

Figure 6 shows the reliability distribution of the quadratic regression equation of yield stress and viscosity. The straight lines in the figure represent the predicted values of the quadratic regression equation for yield stress and viscosity. According to the regression equation, the maximum deviation of yield stress is 11.35%, and the maximum deviation of viscosity is 11.82%, which shows that the quadratic regression equation has a good prediction ability for yield stress and viscosity.

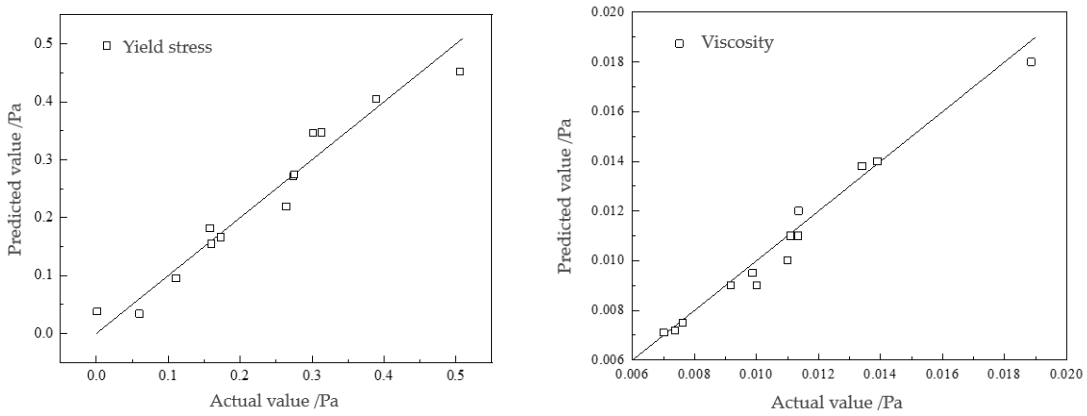

(**a**) (**b**)

Figure 6. Comparison of actual value and predicted values of yield stress and viscosity. (**a**) Comparison of actual value and predicted values of yield stress; and (**b**) comparison of actual value and predicted values of viscosity.

4.3. Significance Analysis of Influencing Factors

To make the slurry more stable, efficient, and energy-saving, it is necessary to study the effects of pipe diameter, particle size, and solid content on yield stress and viscosity by performing variance analysis on the designed BBD model. This analysis method can characterize the significance of each factor of the model, that is, analyze and compare the importance of the influence of a single influence factor (pipe diameter, particle size, or solid content) on the response target (yield stress and viscosity). Tables 5 and 6 show the specific results of yield stress and viscosity variance analysis, where the "freedom degree" represents the number of free variations in the influencing factor, and the "sum of squares" represents the sum of squares of each influencing factor variable. The F-value and *p*-value are the results of the significance test of the model and its coefficients in the analysis of variance. Generally, $p \leq 0.05$ is significant, and $p \leq 0.01$ is highly significant. The data in Tables 5 and 6 were obtained using ANOVA with Design Expert 8.0 software.

Table 5. Variance analysis of response function model for yield stress.

Variance Source	Free. Degree	Sum of Squares	F-Value	*p*-Value	Significance
regression equation	9	2.200×10^{-1}	15.260	0.0008	Highly significant
D	1	9.200×10^{-2}	56.740	0.0001	Highly significant
d	1	1.800×10^{-2}	11.400	0.0118	Significant
C_v	1	7.600×10^{-2}	47.200	0.0002	Highly significant

Table 6. Variance analysis of the response function model of viscosity.

Variance Source	Free. Degree	Sum of Squares	F-Value	*p*-Value	Significance
Model	9	1.249×10^{-4}	47.76	<0.0001	Highly significant
D	1	1.240×10^{-5}	42.68	0.0003	Highly significant
d	1	3.521×10^{-5}	121.20	<0.0001	Highly significant
C_v	1	3.091×10^{-5}	106.39	<0.0001	Highly significant

4.3.1. Yield Stress

From Table 5, the *p*-value of the model is 0.0008. This shows that the quadratic regression equation of yield stress obtained by fitting is highly significant, and there is a nonlinear relationship between the response value and the influence factor. Among them, the primary term pipe diameter D, particle diameter d, and solid content C_v have a significant impact on the yield stress. For the yield stress, the larger the F-value, the more significant the influence of this factor. Therefore, the main influence factor of the slurry yield stress is the pipe diameter, followed by the solid content, and finally, the particle size.

The variation in yield stress with pipe diameter and solid content, indirectly obtained by analyzing the rheological properties of the slurry according to the experimental pressure drop, is shown in Figure 7a. The yield stress increases with increasing pipe diameter and solid content. This is because, under the same solid content, the distribution of solid particles in the small pipe diameter is greater (more dispersed) than that in the larger pipe diameter. The solid particles in the small pipe diameter do not completely gather in the upper half area, and the internal friction force is smaller, so the yield stress is also smaller. The increase in solid content increases the overall viscosity of the ice slurry, increases the flow resistance, and thus increases the yield stress. When the pipe diameter and solid content are the same, the change in yield stress with particle size is not linear (Figure 7b). The yield stress of each particle size at the same solid content fluctuates around a value. Therefore, according to the regression analysis theory, compared with the pipe diameter and solid content, the particle size variable has less influence on the yield stress.

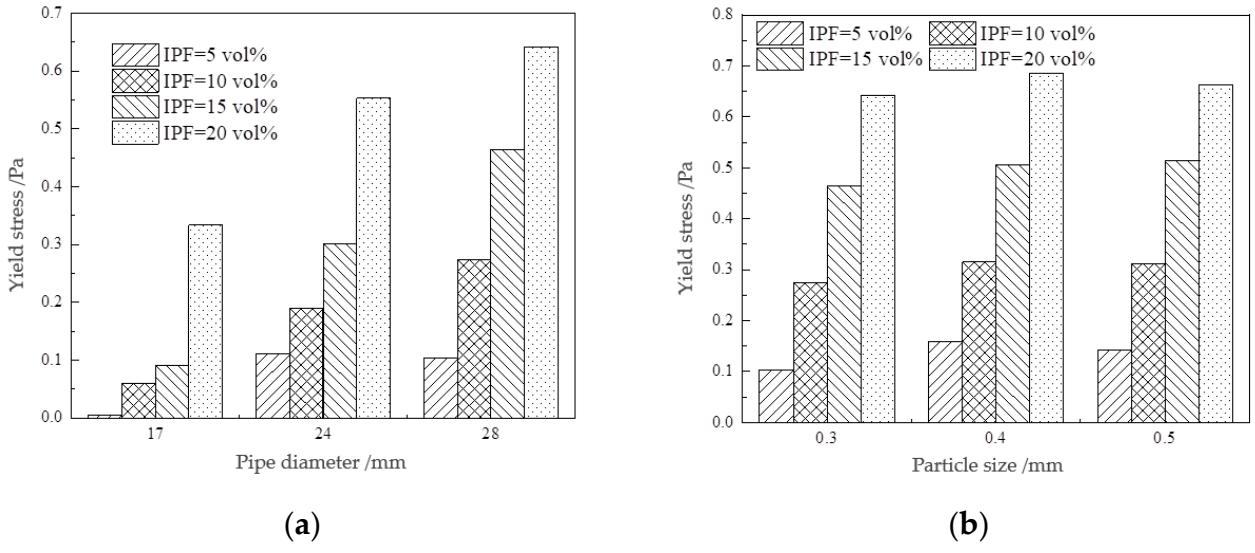

Figure 7. Factors affecting yield stress. (**a**) The relationship between yield stress and pipe diameter; and (**b**) the relationship between yield stress and particle size.

4.3.2. Viscosity

From Table 6, the model *p*-value is less than 0.0001. It shows that the fitted viscosity quadratic regression equation is highly significant, and there is a nonlinear relationship between the response value and the influence factor. Among them, pipe diameter, particle size, and solid content have highly significant effects on viscosity. According to the value of F, for viscosity, the primary and secondary relationship of the importance of the influencing factors is particle size > solid content > pipe diameter.

As shown in Figure 8a, under the same solid content, there is no obvious increase or decrease in viscosity with the change in pipe diameter, and it basically remains close to a certain value. Therefore, the influence of pipe diameter on viscosity is small. As shown in Figure 8b, using the same pipe diameter, the viscosity increases with increasing particle size and increases with increasing solid content. This is because the larger the particle size of solid particles, the greater the resistance caused by the interaction between solid particles, and, therefore, the viscosity increases. The increase in solid content makes the collision between solid particles more frequent, and intensifies the friction between solid particles, so the viscosity increases. At the same time, it can also be found that when the solid content is 5 vol% and 10 vol%, the viscosity changes little, that is, the shear thickening phenomenon is more likely to occur in the thicker dispersion system. Therefore, in the case of low solid content, the slurry flows more easily and the flow resistance is less, that is, the viscosity is lower.

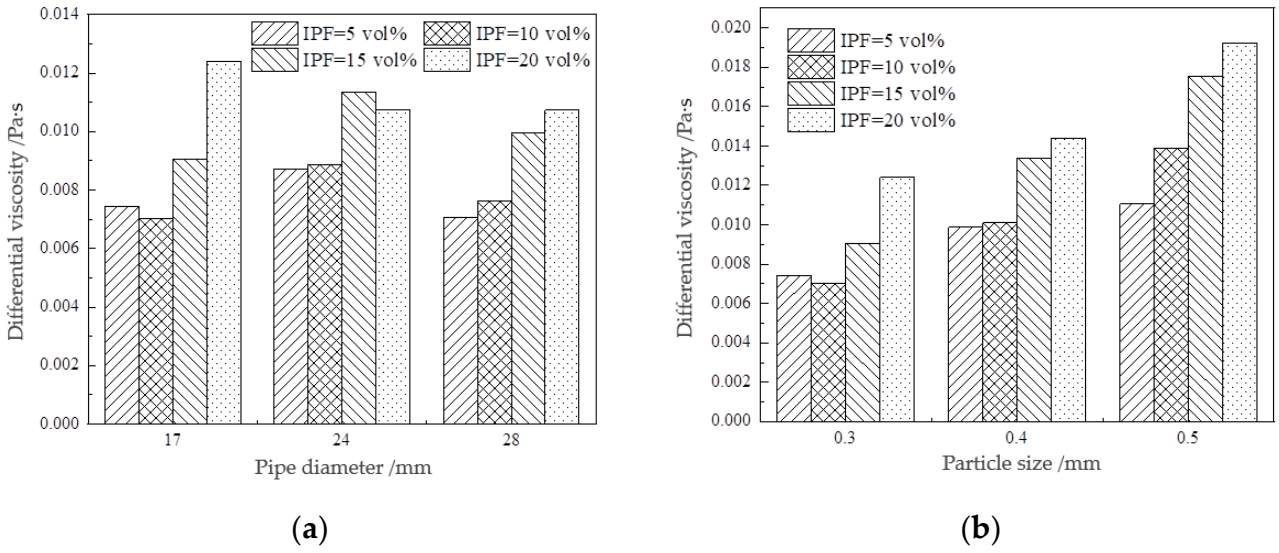

Figure 8. Factors affecting viscosity. (**a**) The relationship between viscosity and pipe diameter; and (**b**) the relationship between viscosity and particle size.

4.4. Analysis of Coupling Effect of Influencing Factors

Through variance analysis, the significant influence of a single factor on yield stress and viscosity was obtained. Next, the influence of the coupling effect of pipe diameter, particle size, and solid content on rheological parameters was analyzed using the response surface graphs. According to the quadratic regression equation model, the response surface graphs under different factors were obtained. These graphs can directly reflect the influence of various factors on yield stress and viscosity and the interaction of various factors in terms of rheological behavior. Among them, the slope in the 3D surface map reflects the degree of influence of various factors. If the slope is steep, it indicates that this factor has a significant impact on the response value. The rheological properties of mixed slurry are mainly affected by three factors: pipe diameter, particle size, and solid content. Response surface graphs of the effects of the interactions between every two factors on yield stress and viscosity are shown in Figures 9 and 10.

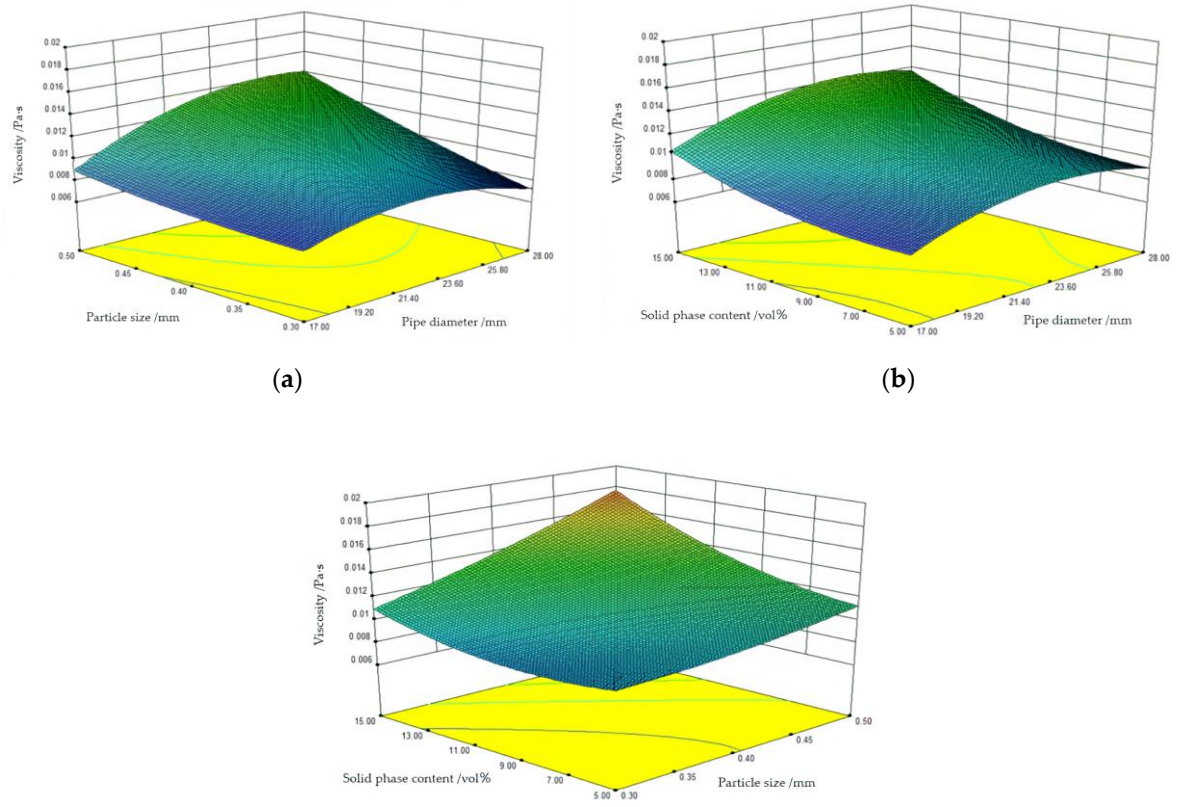

Figure 9. Response surface graphs of the interaction of three factors to yield stress. (**a**) The effect of pipe diameter and particle size on yield stress; (**b**) The effect of pipe diameter and solid content on yield stress; and (**c**) The effect of particle size and solid content on yield stress.

As shown in Figure 9, with an increase in pipe diameter, particle size, and solid content, the slope of the curved surface gradually inclines. However, the slope of pipe diameter and solid content is relatively larger, indicating that the most significant interaction between the two factors is pipe diameter and solid content. This is consistent with the analysis of variance in the quadratic regression equation. The second most significant factor is particle size and solid content, and the least significant factor is pipe diameter and particle size. Therefore, in order to reduce the yield stress of ice slurry, the pipe diameter and solid content should be given priority.

As shown in Figure 10, for viscosity, with an increase in pipe diameter, particle size, and solid content, the slope of the curved surface gradually inclines. The most significant factor that interacts with each other is particle size and solid content; the more significant factor is pipe diameter and particle size, and the least significant factor is pipe diameter and solid content. Therefore, in order to reduce the viscosity of the mixed slurry, priority should be given to the solid content and particle size.

Figure 8a,b shows that under some working conditions, the relationship between viscosity and solid content is not monotonic. Therefore, it is difficult to select the working condition with the minimum viscosity throughout the experiments. The most significant influencing factors on yield stress are pipe diameter and solid content, and the most significant influencing factors on viscosity are particle size and solid content. According to the response surface graphs (Figures 9b and 10c), the working conditions with the minimum yield stress and viscosity within the range of experimental working conditions are listed in Table 2. The working conditions with the minimum yield stress and viscosity are a pipe diameter of 17 mm, a particle size of 0.3 mm, and a solid content of 7.76 vol%. In these

conditions, the yield stress is 7.19×10^{-5} Pa and the viscosity was 0.0074 Pa·s. In addition, according to the experimental measurement results (Figure 5 and Table 4), the smaller the pipe diameter, the smaller the yield stress. The smaller the particle size, the smaller the viscosity. This is consistent with the conclusion of the best operating condition for the mixed slurry obtained by the response surface method. With experimental conditions of a pipe diameter of 17 mm, a particle size of 0.3 mm, and a solid content of 10 vol%, the measured viscosity was 0.00762 Pa·s, which is also consistent with the best operating conditions of the mixed slurry obtained using the response surface method.

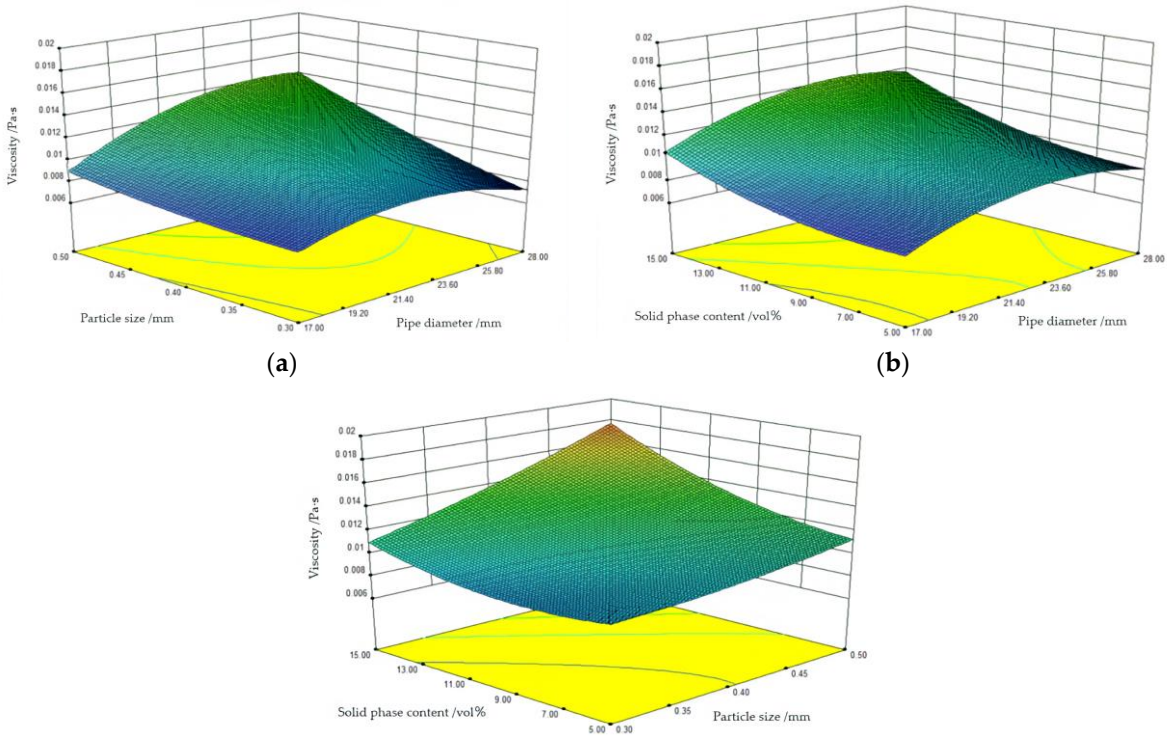

Figure 10. Response surface graphs for the interaction of three factors on viscosity. (**a**) The effect of pipe diameter and particle size on viscosity; (**b**) The effect of pipe diameter and solid content on viscosity; and (**c**) The effect of particle size and solid content on viscosity.

5. Conclusions

In this paper, polyethylene particles with similar density to ice crystal particles were selected to simulate the flow process of ice slurry in a pipe, effectively controlling the size of the particle size and avoiding the impact of a series of dynamic behaviors of ice crystal particles. Based on the rheological model of mixed slurry determined by the experiment, the response surface optimization design method was used for yield stress and viscosity, and the quadratic regression equation was determined for variance analysis. At the same time, the interaction between various factors was analyzed through a response surface graph, and the following conclusions were obtained:

1. When the solid content, particle size, and pipe diameter were fixed, the shear stress measured in the experiment increased with increasing shear rate, and there was an intercept on the Y-axis. Therefore, the H–B model could be used for the regression analysis of the rheological properties of the light-particle mixed paste. The rheological index n of the slurry was always greater than 1, which indicated that the rheological relationship of the mixed slurry was an expansive plastic fluid with yield stress.

2. The primary and secondary relationships of factors (pipe diameter, particle size, solid content) affecting the rheological parameters (yield stress and viscosity) were comprehensively analyzed using the response surface method. According to the experimental results, the response function satisfying the quadratic regression equation was obtained. The prediction deviation of the response function for yield stress and viscosity was less than 11.82%. The variance analysis of the response function showed that the influence of each factor on the yield stress is in the order of pipe diameter, solid content, and particle size. The yield stress increases with increasing pipe diameter and solid content but does not change with the particle size. The influence degree of each factor on viscosity from large to small is as follows: particle size, solid content, and pipe diameter. The viscosity increases with increasing particle size and increasing solid content and does not change significantly with the pipe diameter. When the pipe diameter is fixed, the solid content increases from 5 vol% to 10 vol%, which has little effect on viscosity. It shows that the shear thickening phenomenon is more likely to occur in the thicker dispersion system. The analysis of the sensitivity of multifactor interaction in the response surface graphs showed that the interaction of pipe diameter and solid content had the most significant impact on yield stress. The interaction of particle size and solid content had the most significant effect on viscosity.
3. The response surface method is proposed as a method to determine the energy-saving transportation conditions, and the rationality of the method is verified by experiments, which provides a reference for the optimization of the design of light-particle slurry transportation.

Author Contributions: Conceptualization, X.W. and L.Z.; methodology, X.W. and L.Z.; software, X.W. and F.W.; validation, X.W., F.W., J.L. and Y.Z.; formal analysis, L.Z.; investigation, X.W. and L.Z.; resources, X.W. and L.Z.; data curation, X.W., F.W., J.L. and Y.Z.; writing—original draft preparation, X.W. and F.W.; writing—review and editing, X.W. and L.Z.; visualization, X.W. and F.W.; supervision, X.W.; project administration, X.W. and L.Z.; funding acquisition, X.W., J.L. and L.Z. All authors have read and agreed to the published version of the manuscript.

Funding: This research was supported by the Suzhou Science and Technology Development Project (SNG2020054), Jiangsu Natural Science Foundation Project (BK20190944), and the Jiaxing Science and Technology Project (2021AY10055).

Data Availability Statement: The data that support the findings of this study are available from the corresponding author.

Conflicts of Interest: The authors declare no conflict of interest.

References

1. Long, Y.; Wang, S.; Wang, J.; Zhang, T. Numerical and analytical investigations of heat transfer for a finned tube heat exchanger with ice slurry as cooling medium. *Sci. Technol. Built Environ.* **2017**, *23*, 478–489. [CrossRef]
2. Kauffeld, M.; Wang, M.; Goldstein, V.; Kasza, K. Ice slurry applications. *Int. J. Refrig.* **2010**, *33*, 1491–1505. [CrossRef]
3. Davies, T.W. Slurry ice as a heat transfer fluid with a large number of application domains. *Int. J. Refrig.* **2005**, *28*, 108–114. [CrossRef]
4. Kalaiselvam, S.; Karthik, P.; Ranjit, R.S. Numerical investigation of heat transfer and pressure drop characteristics of tube–fin heat exchangers in ice slurry HVAC system. *Appl. Therm. Eng.* **2009**, *29*, 1831–1839. [CrossRef]
5. Kauffeld, M.; Gund, S. Ice slurry–History, current technologies and future developments. *Int. J. Refrig.* **2019**, *99*, 264–271. [CrossRef]
6. Dodoo, A.; Ayarkwa, J. Effects of climate change for thermal comfort and energy performance of residential buildings in a Sub-Saharan African climate. *Buildings* **2019**, *9*, 215. [CrossRef]
7. Kirilovs, E.; Zotova, I.; Gendelis, S.; Jörg-Gusovius, H.; Kukle, S.; Stramkale, V. Experimental study of using micro-encapsulated phase-change material integrated into hemp shive wallboard. *Buildings* **2020**, *10*, 228. [CrossRef]
8. Bellas, I.; Tassou, S.A. Present and future applications of ice slurries. *Int. J. Refrig.* **2005**, *28*, 115–121. [CrossRef]
9. Ayel, V.; Lottin, O.; Peerhossaini, H. Rheology flow behaviour and heat transfer of ice slurries: A review of the state of the art. *Int. J. Refrig.* **2003**, *26*, 95–107. [CrossRef]
10. Rayhan, F.A.; Yanuar; Pamitran, A.S. Effect of ice mass fraction on ice slurry flow for cold energy storage application. *Energy Rep.* **2020**, *6*, 790–794. [CrossRef]

11. Mellari, S.; Boumaza, M.; Egolf, P.W. Physical modeling, numerical simulations and experimental investigations of Non-Newtnian ice slurry flows. *Int. J. Refrig.* **2012**, *35*, 1284–1291. [CrossRef]
12. Monteiro, A.C.S.; Bansal, P.K. Pressure drop characteristics and rheological modeling of ice slurry flow in pipes. *Int. J. Refrig.* **2010**, *33*, 1523–1532. [CrossRef]
13. Onokoko, L.C.; Galanis, N.; Poirier, M.; Poncet, M. Rheology of a propylene-glycol ice slurry. In Proceedings of the 26th CANCAM, Victoria, BC, Canada, 29 May—1 June 2017.
14. Mika, L. Rheological behaviour of low fraction ice slurry in pipes and pressure loss in pipe sudden contractions and expansions. *Int. J. Refrig.* **2012**, *35*, 1697–1708. [CrossRef]
15. Illán, F.; Viedma, A. Experimental study on pressure drop and heat transfer in pipelines for brine based ice slurry Part II: Dimensional analysis and rheological model. *Int. J. Refrig.* **2009**, *32*, 1024–1031. [CrossRef]
16. Arellano, M.; Benkhelifa, H.; Alvarez, G.; Flick, D. Coupling population balance and residence time distribution for the ice crystallization modeling in a scraped surface heat exchanger. *Chem. Eng. Sci.* **2013**, *102*, 502–513. [CrossRef]
17. Pronk, P.; Ferreira, C.A.I.; Witkamp, G.J. A dynamic model of Ostwald ripening in ice suspensions. *J. Cryst. Growth* **2005**, *275*, 1355–1361. [CrossRef]
18. Kumano, H.; Hirata, T.; Hagiwara, Y.; Tamura, F. Effects of storage on flow and heat transfer characteristics of ice slurry. *Int. J. Refrig.* **2012**, *35*, 122–129. [CrossRef]
19. Chai, X.; Xu, L.; Sun, Y.; Liang, Z.; Lu, E.; Li, Y. Development of a cleaning fan for a rice combine harvester using computational fluid dynamics and response surface methodology to optimise outlet airflow distribution. *Biosyst. Eng.* **2020**, *192*, 232–244. [CrossRef]
20. Zhu, L.L.; Jin, Z.H.; Zhao, Y.; Duan, Y. Rheological properties of cemented coal gangue backfill based on response surface methodology. *Constr. Build. Mater.* **2021**, *306*, 124836. [CrossRef]
21. Alkalbani, A.M.; Chala, G.T.; Myint, M.T.Z. Experimental investigation of rheological properties of water-base mud with zinc oxide nanoparticles using response surface methodology. *J. Pet. Sci. Eng.* **2022**, *208*, 109781. [CrossRef]
22. Egolf, P.W.; Kauffeld, M. From physical properties of ice slurries to industrial ice slurry applications. *Int. J. Refrig.* **2005**, *28*, 4–12. [CrossRef]